Polyhedron 50 (2013) 556–570

Contents lists available at SciVerse ScienceDirect

Polyhedron

journal homepage: www.elsevier.com/locate/poly

Syntheses, structures and photoluminescent properties of a series of divalent nickel and cadmium complexes based on 3-carboxy-1-(4′-(2″-carboxy) biphenylmethyl)-2-oxidopyridinium and structurally different N-donor ligands

Ai-Ting Pu, Jin Yang *, Wei-Qiu Kan, Yan Yang, Jian-Fang Ma *

Key Lab of Polyoxometalate Science, Department of Chemistry, Northeast Normal University, Changchun 130024, People's Republic of China

ARTICLE INFO

Article history:
Received 11 August 2012
Accepted 29 November 2012
Available online 7 December 2012

Keywords:
Coordination polymers
Topological structure
Luminescence

ABSTRACT

Ten new coordination polymers, namely, $[Cd(L)(pbib)_{0.5}]$ (**1**), $[Ni(L)(pbib)]\cdot 2H_2O$ (**2**), $[Cd_2(L)_2(pytp)_2]\cdot H_2O$ (**3**), $[Cd(L)(tbpy)]$ (**4**), $[Ni(L)(pytp)]$ (**5**), $[Ni(L)(tbpy)]\cdot 0.25H_2O$ (**6**), $[Cd(L)(biim\text{-}6)_{0.5}]$ (**7**), $[Cd(L)(phen)]$ (**8**), $[Cd_3(L)_3(H_2O)]\cdot H_2O$ (**9**), and $[Cd_3(L)_3(biim\text{-}4)_{0.5}]\cdot 6H_2O$ (**10**), where biim-4 = 1,1′-(1,4-butanediyl)bis(imidazole), biim-6 = 1,1′-(1,6-hexanedidyl)bis(imidazole), pbib = 1,4-bis(imidazol-1-ylmethyl)benzene, phen = 1,10-phenanthroline, pytp = 2-(6′-(pyridin-2″-yl)-4′-p-tolylpyridin-2′-yl)pyridine, tbpy = 2-(4′-(4″-tert-butylphenyl)-6′-(pyridin-2″-yl)pyridin-2′-yl)pyridine and H_2L = 3-carboxy-1-(4′-(2″-carboxy) biphenylmethyl)-2-oxidopyridinium, have been synthesized under hydrothermal conditions. Their structures have been determined by single-crystal X-ray diffraction analyses and further characterized by infrared spectra (IR), elemental analyses, powder X-ray diffraction (PXRD) and thermogravimetric (TG) analyses. Compounds **1** and **2** show layer structures. Neighboring layers are further linked by π–π stacking interactions to form 3D supramolecular architectures. Compound **3** consists of two crystallographically different dimers, which are further linked by π–π and hydrogen-bonding interactions into a 2D supramolecular architecture. Compounds **4**–**6** feature chain structures. In **4**, neighboring chains are stacked by π–π interactions to result in a 2D supramolecular architecture. In **5**, the adjacent chains are linked by π–π interactions to yield a 3D supramolecular architecture. In **6**, neighboring chains are further linked by hydrogen-bonding interactions into a 3D supramolecular architecture. Compound **7** exhibits a 2D 6^3-**hcb** network. Neighboring networks are further extended by π–π stacking interactions into a 3D supramolecular architecture. Compound **8** displays a (4,4) sheet. Compound **9** reveals a 2D (4,4) network. Compound **10** shows a 3D 5-connected framework with $(4^6\cdot 6^4)$ topology. The effects of the L anions and the N-donor ligands on the structures of the coordination polymers have been discussed. In addition, the luminescent properties of **1**, **3**, **4** and **7**–**10** have also been investigated in details.

1. Introduction

Currently, considerable efforts have been focused on the design and synthesis of novel multidimensional coordination polymers not only because of their intriguing variety of architectures and topologies but also because of their enormous potential applications in the fields of electrical conductivity, magnetism, nonlinear optics, ion exchange, and gas absorption [1]. Nevertheless, it is still a great challenge to predict the structures and properties of the target coordination polymers [2]. Usually, the construction of the coordination polymers can be influenced by several factors, such as the nature of the anions, N-donor ligands, the central metals, pH values, and reaction temperatures [3,4]. Among these factors, the anions play a key role in the design and construction of various coordination polymers. In this regard, the multicarboxylate ligands, as an important type of organic anions, have been extensively utilized as multifunctional linkers because of their rich coordination modes in the assembly of polymeric structures, such as monodentate, bidentate and tridentate [5]. Up to now, benzene–polycarboxylate anions such as benzene–tricarboxylic acid and benzene–tetracarboxylic acid have been widely studied in the construction of coordination polymers [6]. However, flexible pyridine-carboxylate ligands have received less attention [7].

Based on above consideration, a new flexible dicarboxylic acid ligand 3-carboxy-1-(4′-(2″-carboxy)biphenylmethyl)-2-oxidopyridinium (H_2L) was synthesized (Scheme 1). The H_2L ligand was chosen as the organic ligand based on the following considerations: (i) The H_2L ligand contains a $-CH_2-$ spacer at the center

---

* Corresponding authors. Fax: +86 431 85098620 (J.-F. Ma).
E-mail addresses: yangjinnenu@yahoo.com.cn (J. Yang), jianfangma@yahoo.com.cn (J.-F. Ma).

0277-5387/$ - see front matter © 2012 Elsevier Ltd. All rights reserved.
http://dx.doi.org/10.1016/j.poly.2012.11.045

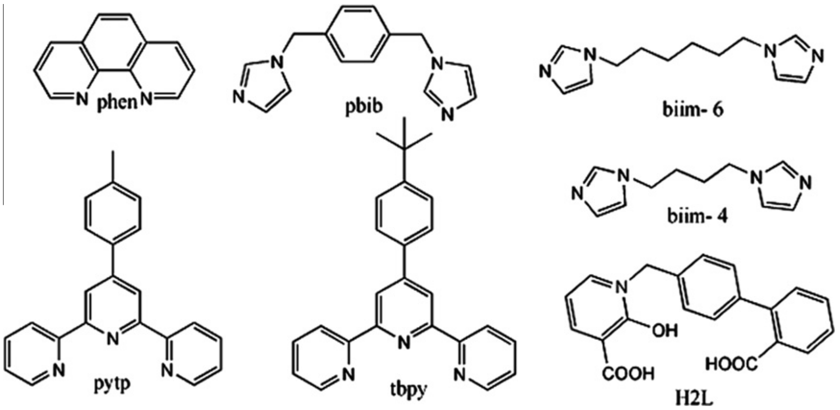

Scheme 1. Structures of H_2L and the N-donor ligands used in this work.

of the molecule. Therefore, the biphenyl and pyridine rings can freely twist to meet the requirements of the coordination geometries of metal cations in different directions, offering various possibilities for construction of frameworks with unique structures. (ii) The H_2L ligand is a multidentate ligand because of the presence of two carboxylate groups and one hydroxyl group. The carboxylate and hydroxyl oxygen groups can adopt varied coordination modes with metal cations (Scheme 2).

In this work, ten new compounds based on flexible H_2L and different N-donor ligands have been synthesized under hydrothermal conditions, namely, $[Cd(L)(pbib)_{0.5}]$ (**1**), $[Ni(L)(pbib)]\cdot 2H_2O$ (**2**), $[Cd_2(L)_2(pytp)_2]\cdot H_2O$ (**3**), $[Cd(L)(tbpy)]$ (**4**), $[Ni(L)(pytp)]$ (**5**), $[Ni(L)(tbpy)]\cdot 0.25H_2O$ (**6**), $[Cd(L)(biim\text{-}6)_{0.5}]$ (**7**), $[Cd(L)(phen)]$ (**8**), $[Cd_3(L)_3(H_2O)]\cdot H_2O$ (**9**), and $[Cd_3(L)_3(biim\text{-}4)_{0.5}]\cdot 6H_2O$ (**10**), where biim-4 = 1,1′-(1,4-butanediyl)bis(imidazole), biim-6 = 1,1′-(1,6-hexanedidyl)bis(imidazole), pbib = 1,4-bis(imidazol-1′-ylmethyl) benzene, phen = 1,10-phenanthroline, pytp = 2-(6′-(pyridin-2″-yl)-4′-p-tolylpyridin-2′-yl)pyridine, and tbpy = 2-(4′-(4″-tert-butylphenyl)-6′-(pyridin-2″-yl)pyridin-2′-yl)pyridine. All the compounds are characterized by X-ray crystallography, infrared spectra (IR), powder X-ray diffraction (PXRD) and thermogravimetric analyses (TG). The effects of the L anions and the N-donor ligands on the structures of the coordination polymers have been discussed [8]. Furthermore, the photoluminescent properties of compounds **1**, **3**, **4** and **7**–**10** have also been investigated.

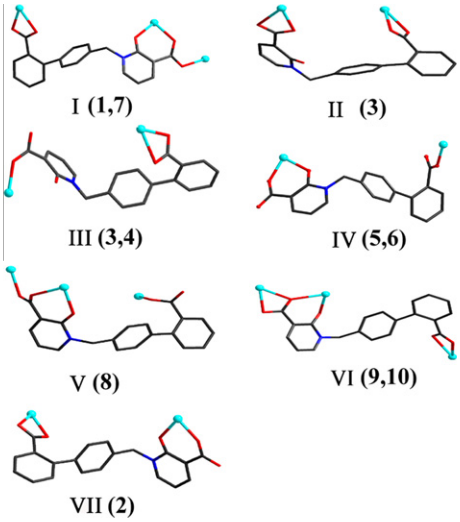

Scheme 2. Coordination modes of the L anions in compounds **1**–**10**.

2. Experimental

2.1. Materials and methods

H_2L and the N-donor ligands were prepared by the procedures reported [9,10]. Other reagents were obtained from commercial suppliers and used without further purification. The C, H and N elemental analyses was conducted on a Perkin–Elmer 240C elemental analyzer. The FT-IR spectra were recorded from KBr pellets in the range 4000–400 cm^{-1} on a Mattson Alpha-Centauri spectrometer. Thermogravimetric analyses (TGA) were performed on a Perkin–Elmer TG-7 analyzer heated from room temperature to 600 °C under nitrogen gas. The solid-state emission/excitation spectra were recorded on a Perkin–Elmer FLS-920 spectrometer. The powder X-ray diffraction (PXRD) data of the samples was collected on a Rigaku Dmax 2000 X-ray diffractometer with graphite monochromatized Cu Kα radiation (λ = 0.154 nm) and 2θ ranging from 5 to 50°. The experimental PXRD patterns are in good agreement with the corresponding simulated ones (Fig. S7 in the Supporting Information). ^{1}H and ^{13}C NMR spectra were recorded on a Bruker UNITY INOVA-500 instrument.

2.2. Synthesis

2.2.1. Synthesis of H_2L

A mixture of 2-hydroxyl nicotinic acid (2.78 g, 20 mmol), concentrated sulfuric acid (2 mL), and EtOH (100 mL) was heated at 90 °C for 8 h. The solvent was evaporated by rotary evaporation to 20 mL, then 200 mL water was added. The mixture was adjusted to pH 7–8 with $NaHCO_3$ powder. The product was extracted by chloroform for three times. The solvent was removed from the filtrate by rotary evaporation, and popcorn solid of 2-hydroxyl nicotinic acid ethyl ester formed immediately.

The 2-hydroxyl nicotinic acid ethyl ester (3.30 g, 20 mmol) and NaOH (0.80 g, 20 mmol) were added to EtOH solution (200 mL), then white solid formed immediately. The mixture was stirred for 1 h, 4-bromomethylbiphenyl-2′-carboxylic acid methyl ester (5.62 g, 20 mmol) and DMF (100 mL) was added. After stirring at 90 °C for 6 h, an excess of NaOH (4.8 g, 120 mmol) and water (50 mL) were added to the mixture stirring at 90 °C for 6 h. The solvent was removed by rotary evaporation, and then 250 mL water was added. The mixture was adjusted to pH 2 with HCl (1.0 mol L^{-1}), and an off-white solid of H_2L formed immediately. The solid was filtered off, washed with water and dried (yield in 94.3%). *Anal.* Calc. for $C_{20}H_{16}NO_5$ (*Mr* = 350.34): C, 68.57; H, 4.60; N, 4.00. Found: C, 68.50; H, 4.45; N, 4.10%. IR data (KBr, cm^{-1}): 3079 (m), 1628 (m), 1559 (w), 1452 (w), 1374 (m), 1304 (s), 1254 (m), 1168 (s), 777 (w), 695 (s). ^{1}H NMR (500 MHz, DMSO) δ/ppm: 5.36 (s, 2H), 6.80 (t, J = 6.0 Hz, 1H), 7.32–7.39 (m, 5H), 7.45 (d, J = 7.5 Hz, 1H), 7.55 (d, J = 7.5 Hz, 1H), 7.72 (d, J = 7.5 Hz, 1H), 8.41–8.47 (m, 2H). ^{13}C NMR (125 MHz, DMSO) δ/ppm: 52.95, 109.35, 117.48, 127.98, 128.18, 129.25, 129.70, 131.03, 131.47, 132.76, 135.13, 140.93, 141.16, 145.71, 146.21, 164.14, 165.28, 170.07.

*2.2.2. Synthesis of [Cd(L)(pbib)$_{0.5}$] (**1**)*

A mixture of $CdCl_2\cdot 2.5H_2O$ (0.011 g, 0.05 mmol), H_2L (0.018 g, 0.05 mmol), pbib (0.012 g, 0.05 mmol), NaOH (0.004 g, 0.1 mmol), methanol (2.6 mL) and water (5.4 mL) was placed in a Teflon reactor, and heated at 140 °C for 3 days. Then it was cooled to room temperature at 10 °C h^{-1}. Colorless block crystals were obtained in a 43% yield. *Anal.* Calc. for $C_{27}H_{20}CdN_3O_5$ (*Mr* = 578.86): C, 56.02; H, 3.48; N, 7.26. Found: C, 56.12; H, 3.38; N, 7.35%. IR data (KBr, cm^{-1}): 3064 (s), 1649 (w), 1579 (w), 1514 (m), 1462 (s), 1394 (w), 1368 (m), 1242 (s), 859 (s), 776 (m), 733 (m), 714 (s).

*2.2.3. Synthesis of [Ni(L)(pbib)]·2H$_2$O (**2**)*

The preparation of **2** was similar to that of **1** except that $NiCl_2\cdot 6H_2O$ was used instead of $CdCl_2\cdot 2.5H_2O$. Pale green crystals of **2** were collected in a 58% yield. *Anal.* Calc. for $C_{34}H_{31}NiN_5O_7$ (*Mr* = 680.35): C, 60.02; H, 4.59; N, 10.29. Found: C, 59.90; H, 4.64; N, 10.40%. IR data (KBr, cm^{-1}): 3063 (s), 2945 (s), 1648 (w), 1583 (w), 1540 (w), 1445 (m), 1408 (w), 1358 (m), 1210 (s), 861 (m), 800 (s), 771 (m).

*2.2.4. Synthesis of [Cd$_2$(L)$_2$(pytp)$_2$]·H$_2$O (**3**)*

A mixture of $CdCl_2\cdot 2.5H_2O$ (0.011 g, 0.05 mmol), H_2L (0.018 g, 0.05 mmol), pytp (0.015 g, 0.05 mmol), NaOH (0.004 g, 0.1 mmol), methanol (2.6 mL) and water (5.4 mL) was placed in a Teflon reactor, which was heated at 140 °C for 3 days, and then it was cooled to room temperature at 10 °C h^{-1}. Colorless block crystals of **3** were obtained in a 30% yield based on Cd(II). *Anal.* Calc. for $C_{84}H_{62}Cd_2N_8O_{11}$ (*Mr* = 1584.22): C, 63.68; H, 3.94; N, 7.07. Found: C, 63.56; H, 3.80; N, 7.19%. IR data (KBr, cm^{-1}): 3061 (s), 1651 (w), 1542 (w), 1443 (m), 1399 (w), 1367 (w), 1249 (m), 1193 (s), 855 (s), 768 (m), 747 (m), 687 (s).

*2.2.5. Synthesis of [Cd(L)(tbpy)] (**4**)*

The preparation of **4** was similar to that of **3** except that tbpy (0.018 g) was used instead of pytp. Methanol (4 mL) and water (4 mL) were placed in a Teflon reactor. Colorless block crystals were obtained in a 53% yield. *Anal.* Calc. for $C_{45}H_{36}CdN_4O_5$ (*Mr* = 825.18): C, 65.50; H, 4.40; N, 6.79. Found: C, 65.62; H, 4.25; N, 6.68%. IR data (KBr, cm^{-1}): 3054 (s), 2964 (m), 1648 (s), 1597 (s), 1545 (s), 1444 (s), 1399 (m), 1364 (m), 1251 (s), 816 (s), 765 (m), 753 (m).

*2.2.6. Synthesis of [Ni(L)(pytp)] (**5**)*

A mixture of $NiCl_2\cdot 6H_2O$ (0.012 g, 0.05 mmol), H_2L (0.018 g, 0.05 mmol), NaOH (0.004 g, 0.1 mmol), and water (8 mL) was placed in a Teflon reactor. The mixture was heated at 150 °C for 3 days. Green crystals of **5** were collected in a 57% yield. *Anal.* Calc. for $C_{42}H_{30}NiN_4O_5$ (*Mr* = 729.41): C, 69.16; H, 4.15; N, 7.68. Found: C, 69.29; H, 4.01; N, 7.79%. IR data (KBr, cm^{-1}): 3056 (s), 2951 (s), 1648 (w), 1595 (w), 1461 (m), 1441 (m), 1387 (w), 1248 (m), 1220 (s), 820 (s), 791 (m), 751 (m).

*2.2.7. Synthesis of [Ni(L)(tbpy)]·0.25H$_2$O (**6**)*

The preparation of **6** was similar to that of **5** except tbpy was used instead of pytp. Green crystals of **6** were collected in a 55% yield). *Anal.* Calc. for $C_{45}H_{36.5}NiN_4O_{5.25}$ (*Mr* = 775.99): C, 69.65; H, 4.74; N, 7.22. Found: C, 69.52; H, 4.65; N, 7.34%. IR data (KBr, cm^{-1}): 3053 (s), 2964 (s), 1644 (w), 1603 (w), 1460 (m), 1440 (m), 1378 (w), 1246 (s), 1217 (s), 820 (s), 792 (m), 751 (m).

*2.2.8. Synthesis of [Cd(L)(biim-6)$_{0.5}$] (**7**)*

A mixture of $CdCl_2\cdot 2.5H_2O$ (0.011 g, 0.05 mmol), H_2L (0.018 g, 0.05 mmol), biim-6 (0.011 g, 0.05 mmol), NaOH (0.004 g, 0.1 mmol), methanol (2.6 mL) and water (5.4 mL) was placed in a Teflon reactor. The mixture was heated at 140 °C for 4 days, and then it was gradually cooled to room temperature. Colorless block crystals were obtained in a 51% yield. *Anal.* Calc. for $C_{26}H_{22}CdN_3O_5$ (*Mr* = 568.87): C, 54.89; H, 3.90; N, 7.39. Found: C, 54.76; H, 3.99; N, 7.51%. IR data (KBr, cm^{-1}): 3056 (s), 2936 (s), 1656 (w), 1545 (w), 1515 (m), 1463 (m), 1394 (w), 1368 (m), 1234 (s), 859 (m), 769 (m), 716 (s).

*2.2.9. Synthesis of [Cd(L)(phen)] (**8**)*

The preparation of **8** was similar to that of **3** except that phen was used instead of pytp. Colorless crystals of **8** were collected in a 56% yield. *Anal.* Calc. for $C_{32}H_{21}CdN_3O_5$ (*Mr* = 639.92): C, 60.06; H, 3.31; N, 6.57. Found: C, 60.18; H, 3.20; N, 6.69%. IR data (KBr, cm^{-1}): 3050 (s), 2936 (s), 1652 (w), 1607 (w), 1576 (w), 1547 (w), 1450 (s), 1400 (m), 1365 (m), 774 (s), 746 (m), 707 (s).

*2.2.10. Synthesis of [Cd$_3$(L)$_3$(H$_2$O)]·H$_2$O (**9**)*

A mixture of $CdCl_2\cdot 2.5H_2O$ (0.011 g, 0.05 mmol), H_2L (0.018 g, 0.05 mmol), NaOH (0.004 g, 0.1 mmol) and water (8 mL) was placed in a Teflon reactor. The mixture was heated at 140 °C for 3 days, and then it was gradually cooled to room temperature. Colorless block crystals were obtained in a 33% yield. *Anal.* Calc. for $C_{60}H_{43}Cd_3N_3O_{17}$ (*Mr* = 1415.17): C, 50.92; H, 3.06; N, 2.97. Found: C, 50.79; H, 3.19; N, 2.82%. IR data (KBr, cm^{-1}): 3613 (s), 3078 (s), 2950 (s), 1648 (w), 1599 (m), 1460 (m), 1398 (w), 1233 (s), 1214 (s), 863 (m), 790 (s), 766 (w).

*2.2.11. Synthesis of [Cd$_3$(L)$_3$(biim-4)$_{0.5}$]·6H$_2$O (**10**)*

The preparation of **10** was similar to that of **9** except that biim-4 was used. Methanol (3 mL) and water (5 mL) were placed in a Teflon reactor. Colorless crystals of **10** were collected in a 57% yield. *Anal.* Calc. for $C_{65}H_{58}Cd_3N_5O_{21}$ (*Mr* = 1582.36): C, 49.34; H, 3.69; N, 4.43. Found: C, 49.46; H, 3.81; N, 4.32%. IR data (KBr, cm^{-1}): 3055 (s), 2950 (s), 1649 (w), 1554 (w), 1460 (m), 1396 (w), 1306 (m), 1233 (m), 879 (s), 861 (m), 763 (m), 720 (s).

2.3. Crystal structure determination

Crystallographic diffraction data for compounds **1**–**10** were recorded on an Oxford Diffraction Gemini R Ultra diffractometer with graphite-monochromated Mo Kα radiation (λ = 0.71073 Å) at 293 K. Absorption corrections were applied using a multi-scan technique. All the structures were solved by direct method of SHELXS-97 and refined by full-matrix least-squares techniques using the SHELXL-97 program within WINGX [11]. All non-hydrogen atoms were easily found from the Fourier difference maps and refined with anisotropic temperature parameters. The disordered atoms C atoms (C25 and C26) for **7** were split over two sites with a total occupancy of 1. Hydrogen atoms attached to carbons were generated geometrically. Hydrogen atoms of the disordered C atoms for **7** could not be positioned geometrically. Hydrogen atoms of O1W for **9** were located from difference Fourier maps and refined with isotropic displacement parameters. Hydrogen atoms of the free water molecules for **2**, **3**, **6**, **9** and **10** were not included in the model. The detailed crystallographic data and structure refinement parameters for these compounds are summarized in Table 1. Selected bond distances and angles and hydrogen bond parameters for them are listed in Tables S1–S10 (see the Supporting Information).

Table 1
Crystal data and structure refinements for compounds **1**–**10**.

	1	**2**	**3**	**4**	**5**	**6**	**7**	**8**	**9**	**10**
Formula	$C_{27}H_{20}CdN_3O_5$	$C_{34}H_{31}NiN_5O_7$	$C_{84}H_{62}Cd_2N_8O_{11}$	$C_{45}H_{36}CdN_4O_5$	$C_{42}H_{30}NiN_4O_5$	$C_{45}H_{36.5}NiN_4O_{5.25}$	$C_{26}H_{22}CdN_3O_5$	$C_{32}H_{21}CdN_3O_5$	$C_{60}H_{43}Cd_3N_3O_{17}$	$C_{65}H_{58}Cd_3N_5O_{21}$
Formula weight	578.86	680.35	1584.22	825.18	729.41	775.99	568.87	639.92	1415.17	1582.36
Crystal system	monoclinic	triclinic	triclinic	monoclinic	monoclinic	monoclinic	monoclinic	orthorhombic	triclinic	triclinic
Space group	$C2/c$	$P\bar{1}$	$P\bar{1}$	$P2_1/n$	$P2_1/n$	$P2_1/c$	$C2/c$	$Pbca$	$P\bar{1}$	$P\bar{1}$
a (Å)	13.8148(6)	10.6610(3)	11.7390(4)	15.635(2)	15.2836(5)	10.7718(4)	15.6300(8)	11.5379(4)	13.982(5)	14.4840(5)
b (Å)	15.8632(6)	10.8820(4)	13.3650(6)	14.6280(18)	8.8648(2)	15.5626(5)	13.7610(5)	16.2173(5)	14.039(5)	15.2760(6)
c (Å)	21.7690(8)	14.4380(6)	23.9190(11)	17.886(3)	25.2366(8)	23.4500(10)	22.2970(9)	27.8815(8)	14.557(5)	17.6280(7)
α (°)	90	109.088(4)	103.391(4)	90	90	90	90	90	101.286(5)	112.514(4)
β (°)	105.131(4)	98.976(3)	90.437(3)	114.791(16)	102.935(3)	101.975(4)	98.446(4)	90	101.660(5)	105.357(3)
γ (°)	90	94.75	101.737(4)	90	90	90	90	90	99.890(5)	93.378(3)
V (Å^3)	4605.2(3)	1547.35(10)	3568.4(3)	3713.7(8)	3332.44(17)	3845.5(3)	4743.7(4)	5217.0(3)	2677.1(16)	3417.7(2)
Z	8	2	2	4	4	4	8	8	2	2
D_{calc} (g/cm^3)	1.670	1.460	1.474	1.476	1.454	1.340	1.593	1.629	1.756	1.538
$F(000)$	2328	708	1612	1688	1512	1618	2296	2576	1408	1590
Goodness-of-fit GOF on F^2	1.050	1.048	1.023	0.999	1.019	1.011	1.034	1.010	1.049	1.016
$^aR_1$ $[I > 2\sigma(I)]$	0.0323	0.0554	0.0486	0.0645	0.0434	0.0540	0.0410	0.0378	0.0381	0.0529
$^bwR_2$ (all data)	0.0745	0.1528	0.1128	0.1301	0.0950	0.1342	0.1016	0.0766	0.0982	0.1614
R_{int}	0.0257	0.0372	0.0383	0.0761	0.0389	0.0434	0.0315	0.0512	0.0269	0.0388

$^aR_1 = \Sigma||F_o| - |F_c||/\Sigma|F_o|$. $^bwR_2 = |\Sigma w(|F_o|^2 - |F_c|^2)|/\Sigma|w(F_o^2)^2|^{1/2}$.

3. Results and discussion

3.1. Crystal structures

3.1.1. Structure of [Cd(L)(pbib)$_{0.5}$] (**1**)

As shown in Fig. 1a, each Cd(II) cation is coordinated by four oxygen atoms from two carboxylate and one phenolic hydroxyl of three L anions (Cd1–O1$^{\#1}$ = 2.228(2), Cd1–O2$^{\#2}$ = 2.305(2), Cd1–O3$^{\#2}$ = 2.310(2), Cd1–O4 = 2.326(2) and Cd1–O5 = 2.388(2) Å) and one N atom from one pbib ligand (Cd1–N2 = 2.314(3) Å) in a distorted octahedral coordination environment. The N2, O2$^{\#2}$, O4 and O5 atoms comprise the basal plane, whereas the O3$^{\#2}$ and O1$^{\#1}$ atoms occupy the axial positions. L anions bridge neighboring Cd(II) cations adopting a μ_3-η^1:η^1:η^1:η^1:η^1 coordination mode (mode I, Scheme 2) to generate an infinite double chain (Fig. 1b). The chains are further linked by pbib ligands to yield a wave-like layer (Fig. S1). Moreover, adjacent layers are extended by face-to-face π–π stacking interactions between imidazole rings with interplanar separation

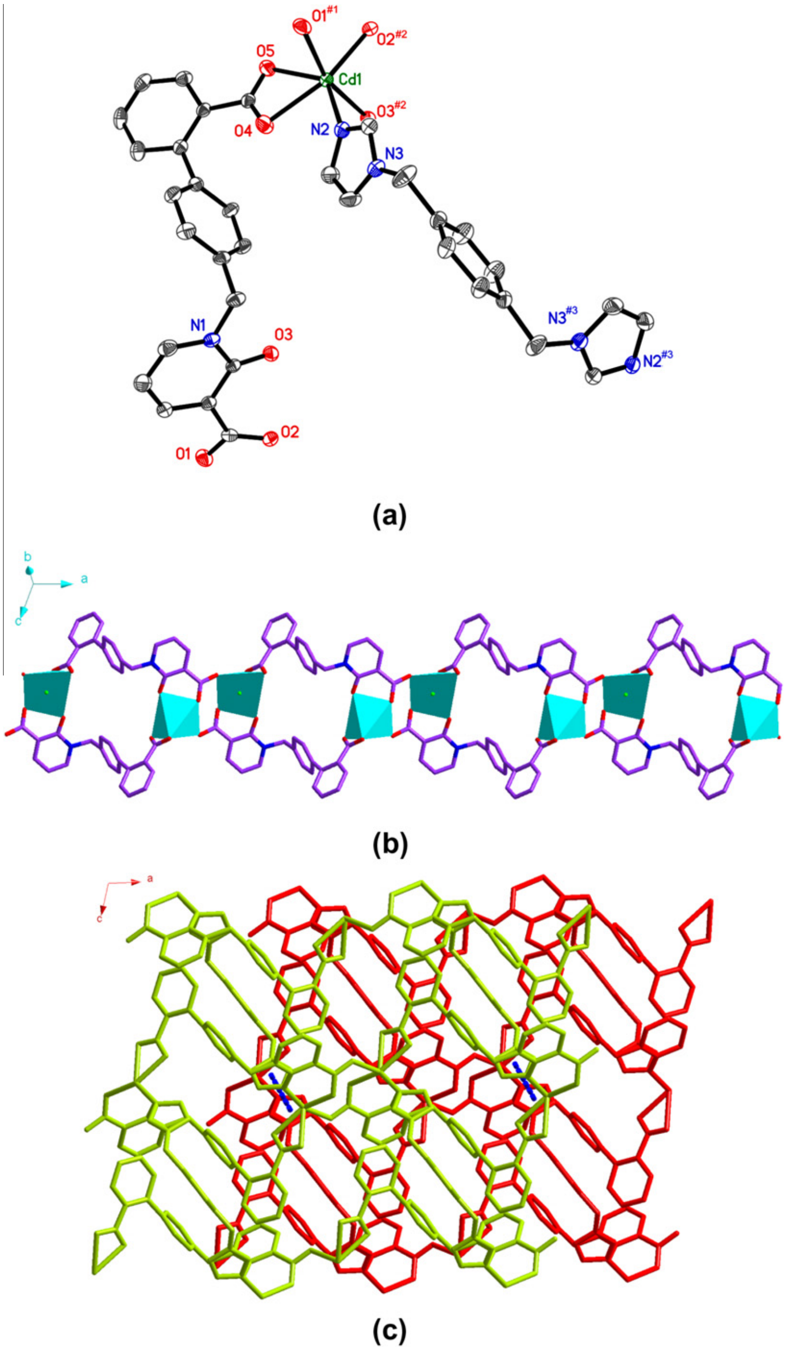

Fig. 1. (a) Coordination environment of the Cd(II) center in compound **1** (thermal ellipsoids are at the 30% probability level). Symmetry codes: $^{\#1}x + 1, y, z$; $^{\#2}-x + 1, -y + 1, -z + 1$; $^{\#3}-x + 1, y, -z + 1/2$; $^{\#4}x - 1, y, z$. (b) View of the infinite double-chain structure constructed by L anions and Cd(II) cations. (c) View of the 3D supramolecular assembly formed by π–π stacking interactions.

being 3.77 Å [12] (the centroid–centroid and slippage distances of 3.89 and 0.94 Å) into a 3D supramolecular architecture (Fig. 1c).

3.1.2. Structure of [Ni(L)(pbib)]·2H$_2$O (**2**)

X-ray crystallography reveals that the asymmetric unit of **2** consists one Ni(II) cation, two halves of pbib ligands, one L anion, and two lattice water molecules (Fig. 2a). Each Ni(II) cation is six-coordinated by two N atoms from two pbib ligands (Ni1–N = 2.078(3)–2.086(3) Å) and four oxygen atoms from two carboxylate and one phenolic hydroxyl of two L anions. The Ni1–O bond lengths are in the range of 2.038(3)–2.236(3) Å, and the O–Ni1–O angles vary from 85.13(11)° to 163.93(11)°. Each L anion bridges two Ni(II) cations in a μ_2-η^1:η^1:η^0:η^1:η^1 coordination mode (mode VII, Scheme 2) to form a dimeric unit [Ni$_2$L$_2$] with the Ni···Ni separation of 9.320 Å. Neighboring [Ni$_2$L$_2$] dimers are linked by one kind of pbib ligand to generate an infinite chain structure (Fig. S2a). The adjacent chains are bridged by another kind of pbib ligand to yield a 2D network (Fig. S2b). The 2D network of **2** can be viewed as a (4^4)-**sql** network structure (Fig. 2b). In addition, the 2D networks are further extended into a 3D supramolecular architecture by π–π stacking interactions between imidazole and benzene rings of L anions with interplanar separation being 3.83 Å (the centroid–centroid and slippage distances of 4.13 and 1.55 Å) (Fig. 2c).

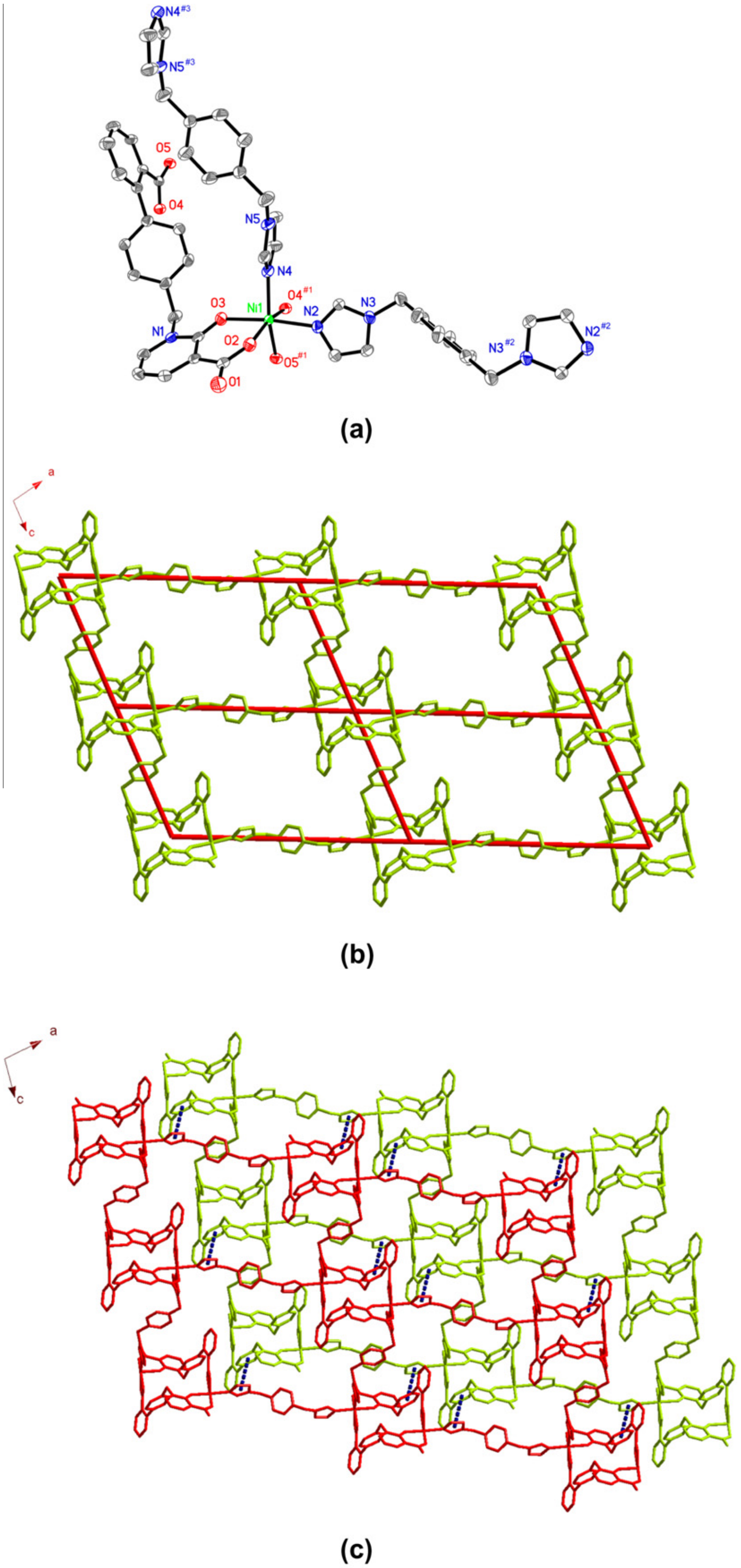

Fig. 2. (a) ORTEP view of **2** showing the local coordination environment of Ni(II) cation with hydrogen atoms and solvent water molecule omitted for clarity (30% probability displacement ellipsoids). Symmetry codes: $^{\#1}-x+2, -y+1, -z+1$; $^{\#2}-x, -y, -z$; $^{\#3}-x+2, -y+1, -z$. (b) Schematic view of the (4^4)-**sql** network structure. (c) View of the 3D supramolecular architecture of **2** formed by π–π stacking interactions.

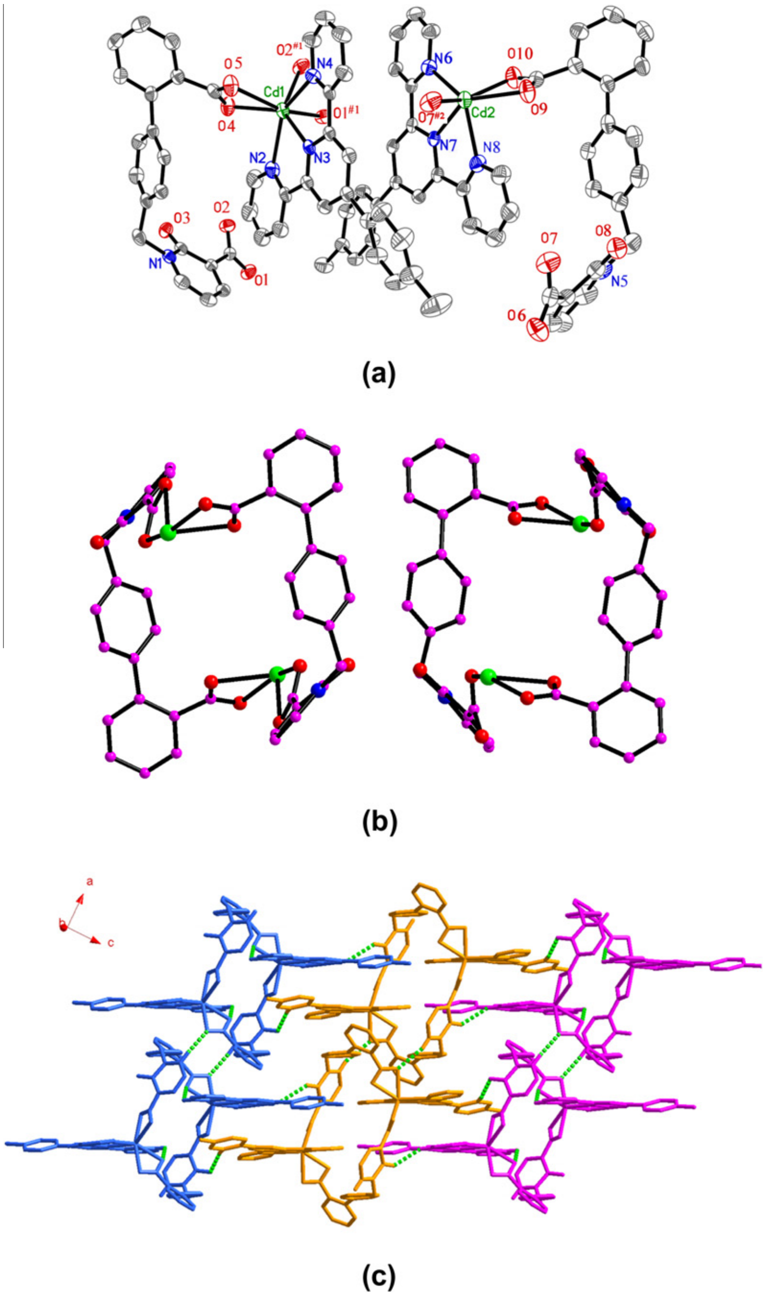

Fig. 3. (a) ORTEP view of **3** showing the local coordination environments of Cd(II) cations with hydrogen atoms omitted for clarity (30% probability displacement ellipsoids). Symmetry codes: $^{\#1}-x+1, -y+1, -z+1$; $^{\#2}-x+2, -y+1, -z+2$. (b) View of the two types of $[Cd_2(L)_2]$ dimeric units (green and red spheres represent Cd(II) and O atoms, respectively). (c) View of the supramolecular layer formed by hydrogen-bonding interactions in **3**. (Color online.)

3.1.3. *Structure of $[Cd_2(L)_2(pytp)_2]\cdot H_2O$ (**3**)*

As illustrated in Fig. 3a, the asymmetric unit of **3** contains two unique Cd(II) cations, two L anions, two pytp ligands and two halves of lattice water molecules. Cd1 cation is seven-coordinated by four oxygen atoms from two carboxylate groups of two L anions (Cd1–O1$^{\#1}$ = 2.469(3), Cd1–O2$^{\#1}$ = 2.323(3), Cd1–O4 = 2.371(3), Cd1–O5 = 2.392(3) Å), and three nitrogen atoms from one pytp ligand (Cd1–N2 = 2.367(4), Cd1–N3 = 2.344(3), Cd1–N4 = 2.384(4) Å) in a distorted pentagonal bipyramid coordination environment. However, Cd2 cation exhibits a distorted octahedral coordination geometry, completed by three oxygen atoms from two carboxylate groups of two L anions and three nitrogen atoms from one pytp ligand. The Cd2–N and Cd2–O bond lengths range from 2.340(4) to 2.375(4) Å and 2.211(3) to 2.391(3) Å, respectively. Cd1 and its symmetry-related species are chelated by two L ligands in μ_2-η^1:η^1:η^1:η^1:η^0 coordination mode to form one type of $[Cd_2(L)_2]$ dimer (mode II, Scheme 2), whereas Cd2 and its symmetry-related species are linked by two L ligands in μ_2-η^1:η^1:η^0:η^1:η^0 coordination mode (mode III, Scheme 2) to yield another type of $[Cd_2(L)_2]$ dimer. The two types of $[Cd_2(L)_2]$ dimers show "O" shaped conformations (Fig. 3b). It is noteworthy that adjacent $[Cd_2(L)_2]$ dimers are linked by two types of face-to-face π–π interactions between pyridine rings of pytp ligands and benzene rings of L anions (face-to-face distances of 3.54 and 3.52 Å, respectively) to generate two unique supramolecular double chain structures (Fig. S3).

In addition, there exist intermolecular C5–H5···O5$^{\#3}$, C32–H32···O8$^{\#2}$, C47–H47···O10$^{\#4}$ and C83–H83···O3$^{\#1}$ hydrogen-bonding interactions (Table S3b), which extend the supramolecular chains into a supramolecular layer (Fig. 3c).

*3.1.4. Structure of [Cd(L)(tbpy)] (**4**)*

The asymmetric unit of **4** contains one crystallographically independent Cd(II) cation, one L anion, one tbpy ligand. As shown in Fig. 4a, each Cd(II) cation is coordinated by three nitrogen atoms from one tbpy ligand (Cd1–N2 = 2.349(5), Cd1–N3 = 2.323(5) and Cd1–N4 = 2.344(5) Å), and three carboxylate oxygen atoms from two L anions (Cd1–O2 = 2.176(5), Cd1–O4$^{\#1}$ = 2.289(5) and Cd1–O5$^{\#1}$ = 2.529(5) Å), showing a distorted octahedral coordination environment. Each L anion bridges two Cd(II) cations in a μ_2-η^1:η^1:η^0:η^1:η^0 coordination mode (mode III, Scheme 2) to form a polymeric helical chain propagating along the crystallographic *c*-axis with a pitch of 14.63 Å (Fig. 4b). The tbpy ligands are attached to the helical chain as tridentate ligands. As shown in Fig. 4c, the tbpy ligands from two neighboring helical chains are well-matched to furnish strong π–π stacking interactions (centroid-to-centroid distance of 3.58 Å and face-to-face distance of 3.30 Å), yielding a supramolecular layer (Fig. 4c). Clearly, the strong π–π stacking interactions play an important role in stabilizing the 2D supramolecular network.

Notably, there are intramolecular and intermolecular hydrogen bonds (C7–H7B···O3, C3–H3···O1$^{\#3}$, C32–H32···O5$^{\#4}$ and C34–H34···O3$^{\#4}$) between the carbon and oxygen atoms of L anions (Table S4b), which further stabilize the supramolecular layer of **4**.

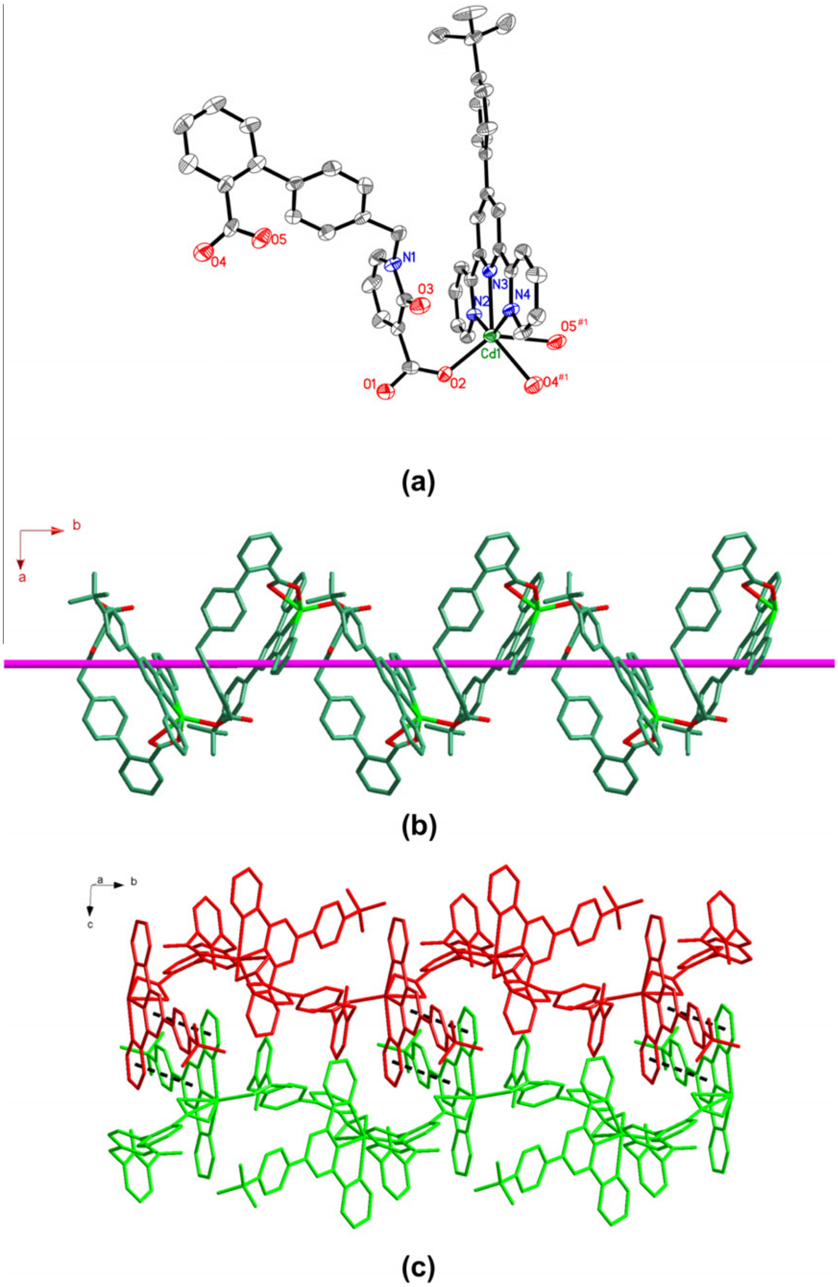

Fig. 4. (a) Coordination environment of the Cd(II) center in compound **4** (30% probability displacement ellipsoids). Symmetry codes for the generated atoms: $^{\#1}-x+3/2$, $y-1/2$, $-z+3/2$; $^{\#2}-x+3/2$, $y+1/2$, $-z+3/2$. (b) View of the helical chain structure. (c) View of the supramolecular layer formed by π–π stacking interactions.

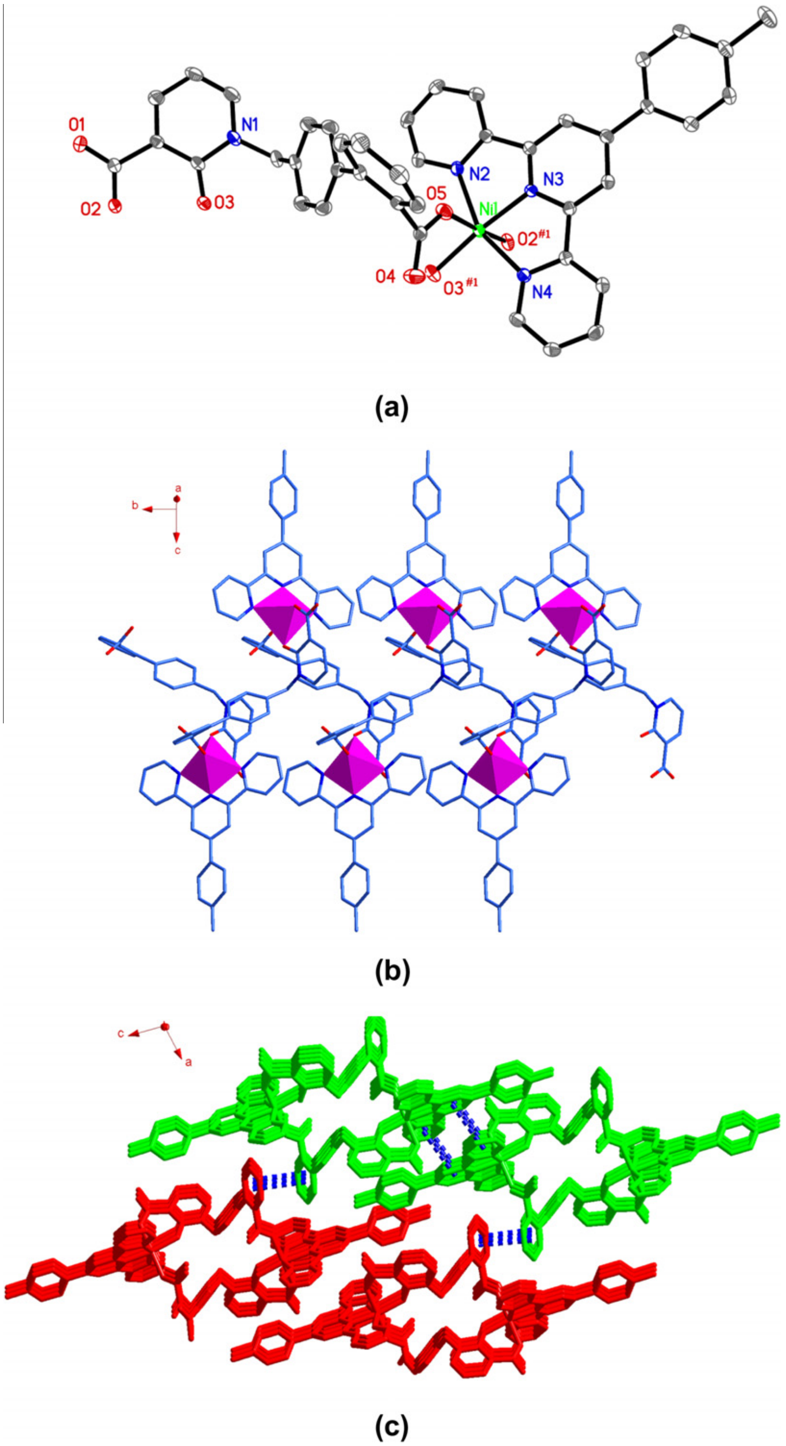

Fig. 5. (a) Coordination environment of the Ni(II) cation in **5** showing 30% thermal probability ellipsoids. Symmetry codes for the generated atoms: $^{\#1}-x + 1/2, y + 1/2, -z + 3/2$; $^{\#2}-x + 1/2, y - 1/2, -z + 3/2$. (b) View of the infinite chain in **5**. (c) View of the 3D supramolecular architecture of **5** formed via π–π stacking interactions.

*3.1.5. Structure of [Ni(L)(pytp)] (**5**)*

As illustrated in Fig. 5a, the asymmetric unit of **5** contains one Ni(II) cation, one L anion and one pytp ligand. Each Ni(II) is six-coordinated by three oxygen atoms from two L anions (Ni1–O2$^{\#1}$ = 2.0501(18), Ni1–O3$^{\#1}$ = 2.0194(18), Ni1–O5 = 2.0287(18) Å), and three nitrogen atoms from one pytp ligand (Ni1–N2 = 2.131(2), Ni1–N3 = 2.001(2) and Ni1–N4 = 2.095(2) Å), exhibiting a distorted octahedral geometry. Each L anion, adopting a μ_2-η^1:η^0:η^0:η^1:η^1 coordination mode (mode IV, Scheme 2), bridges two Ni(II) atoms to form an infinite chain structure. It is interesting to note that the pytp ligands are attached on both sides of the chain (Fig. 5b). Adjacent chains are further linked by two types of face-to-face π–π interactions between two pyridine rings of pytp ligands and two benzene rings of L ligands (face-to-face distances of 3.57 and 3.38 Å, respectively), resulting in a 3D supramolecular architecture (Fig. 5c).

*3.1.6. Structure of [Ni(L1)(tbpy)]·0.25H$_2$O (**6**)*

The asymmetric unit of **6** consists of one Ni(II) cation, one L anion, one tbpy ligand, and a quarter of water molecule. As shown in Fig. 6a, each Ni(II) cation displays a distorted octahedral coordination

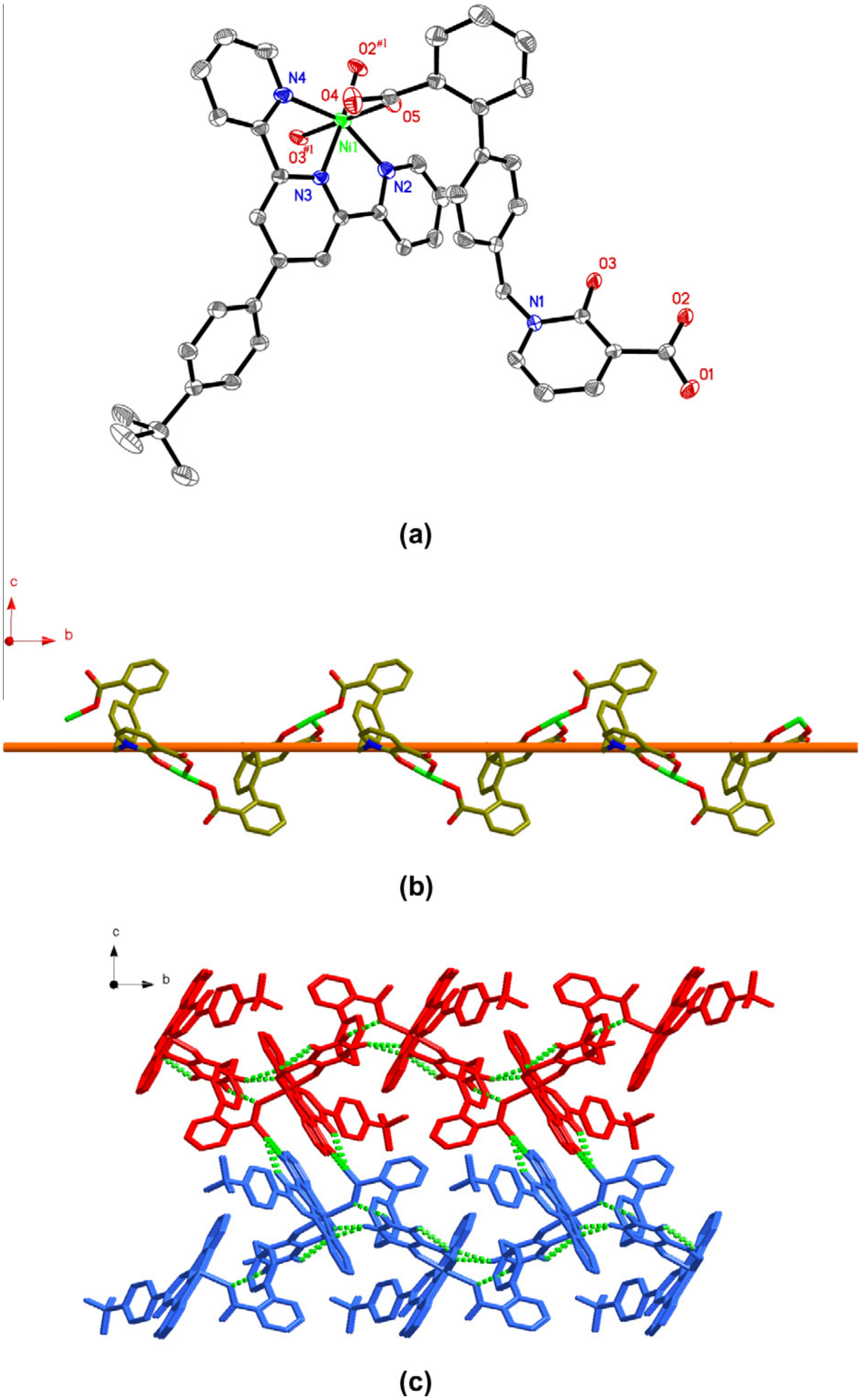

Fig. 6. (a) Coordination environment of the Ni(II) cation in **6** (30% probability displacement ellipsoids). Symmetry codes: $^{\#1}-x+2, y-1/2, -z+1/2$; $^{\#2}-x+2, y+1/2, -z+1/2$. (b) View of the infinite helical-chain constructed by L anions and Ni(II) cations along the *a*-axis. (c) View of the 3D supramolecular architecture of **6** formed via hydrogen-bonding interactions.

geometry, surrounded by three nitrogen atoms from one tbpy ligand (Ni1–N2 = 2.119(3), Ni1–N3 = 1.998(3), Ni1–N4 = 2.110(3) Å) and three oxygen atoms from two L anions (Ni1–O2$^{\#2}$ = 2.007(2), Ni1–O3$^{\#2}$ = 2.072(2) and Ni1–O5 = 2.042(2) Å). Each L anion links two Ni(II) cations in a μ_2-η^1:η^0:η^0:η^1:η^1 coordination mode (mode IV, Scheme 2) to generate an infinite helical chain along the *a*-axis (Fig. 6b). The tbpy ligands, as the dangling arms, are attached on both sides of the chain.

In addition, C29 and C32 from pyridine ring of tbpy ligand donate H atoms to oxygen atoms from carboxyl groups to yield intermolecular C29–H29$\cdots$O4$^{\#5}$ and C32–H32$\cdots$O4$^{\#5}$ hydrogen-bonding interactions. Besides, C4 and C5 from pyridine ring of L ligand donate H atoms to O5$^{\#3}$ and O2$^{\#4}$ atoms to generate intramolecular C4–H4$\cdots$O5$^{\#3}$ and C5–H5$\cdots$O2$^{\#4}$ hydrogen-bonding interactions (Table S6b). These hydrogen bonds join the neighboring chains to from a 3D supramolecular architecture (Fig. 6c).

3.1.7. Structure of $[Cd(L)(biim\text{-}6)_{0.5}]$ (**7**)

As shown in Fig. 7a, the asymmetric unit **7** contains one Cd(II) cation, one-half biim-6 ligand and one L anion. Each Cd(II) cation is six-coordinated by four oxygen atoms from three carboxylate and one phenolic hydroxyl groups of three L anions (Cd1–O1$^{\#1}$ = 2.236(3), Cd1–O2 = 2.277(3), Cd1–O3 = 2.326(3), Cd1–O4$^{\#2}$ = 2.322(3) and Cd1–O5$^{\#2}$ = 2.388(3) Å) and one N atom from one biim-6 ligand (Cd1–N2 = 2.270(4) Å) in a distorted octahedral coordination geometry. As shown in Fig. S4a, adjacent Cd(II) cations are bridged by L anions in μ_3-η^1:η^1:η^1:η^1:η^1 coordination mode (mode I, Scheme 2) to yield a double-chain structure. The chains are linked by the biim-6 ligands to furnish a wave-like layer. The topology of this network can be described as a 3-connected hexagonal honeycomb 6^3-**hcb** net (Figs. S4b and 7b).

In addition, those wavelike layers are further extended into a 3D supramolecular architecture by the face-to-face π–π stacking interactions between imidazole rings of the adjacent layers with the interplanar separation being 3.57 Å (the centroid–centroid and slippage distances of 3.73 and 1.05 Å, respectively). Obviously, the non-covalent π–π stacking interactions play an important role in the formation of the 3D supramolecular structure of **7** (Fig. 7c).

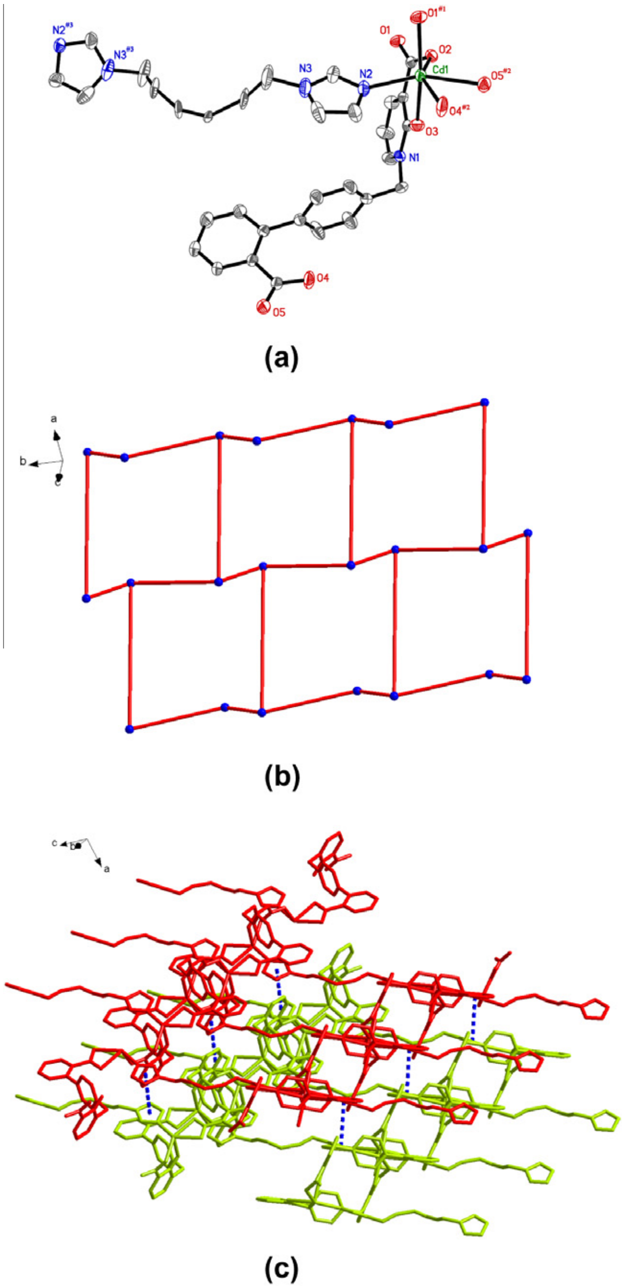

Fig. 7. (a) Coordination environment of the Cd(II) cation in **7** showing 30% thermal probability ellipsoids. Symmetry codes for the generated atoms: $^{\#1}-x+1/2, -y+1/2, -z+1$; $^{\#2}-x+1/2, -y+3/2, -z+1$; $^{\#3}-x+1, y, -z+1/2$. (b) Topological representation of the 6^3-**hcb** net. (c) View of the 3D supramolecular structure of **7** formed via π–π interactions.

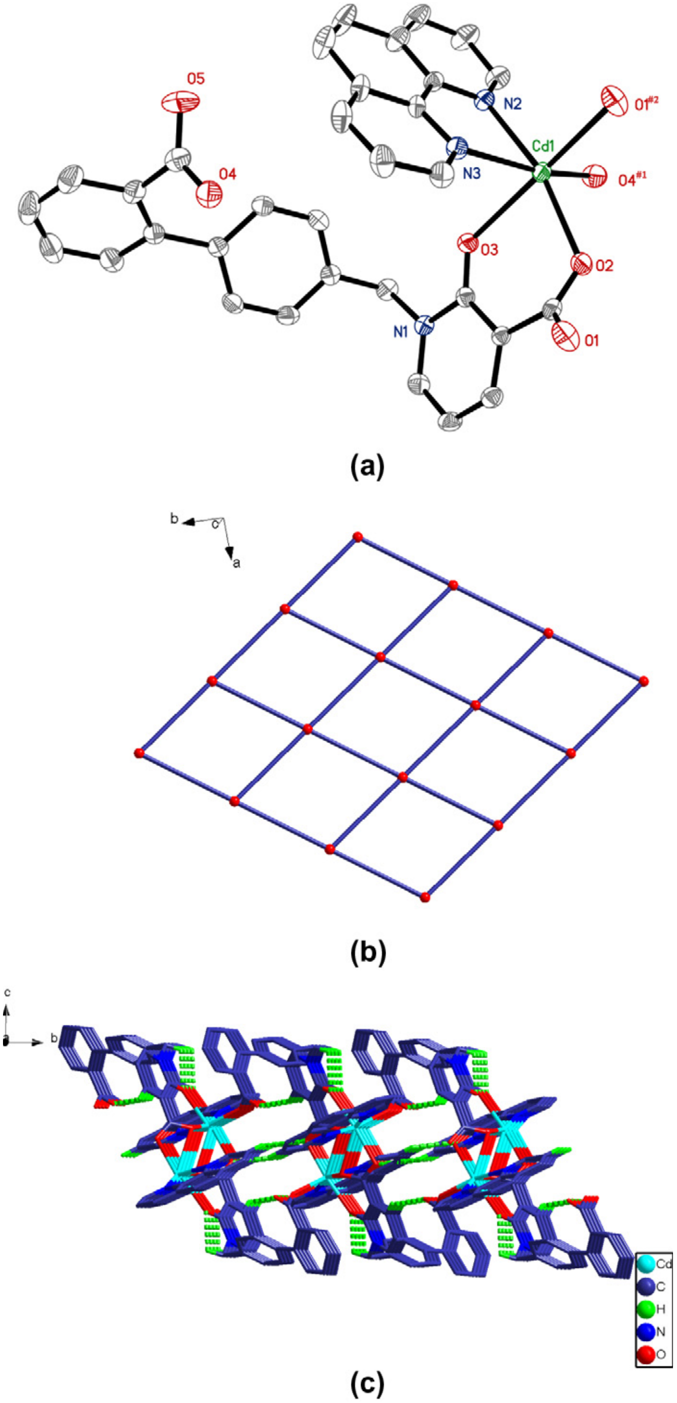

Fig. 8. (a) ORTEP diagram showing the coordination environment for Cd(II) cation in **8**. All H atoms are omitted for clarity. (Symmetry codes: $^{\#1}-x+1/2, y+1/2, z$; $^{\#2}-x, -y, -z+1$; $^{\#3}-x+1/2, y-1/2, z$). (b) View of the 2D (4,4) network of **8**. (c) View of the intramolecular hydrogen-bonding interactions in the 2D structure of **8**.

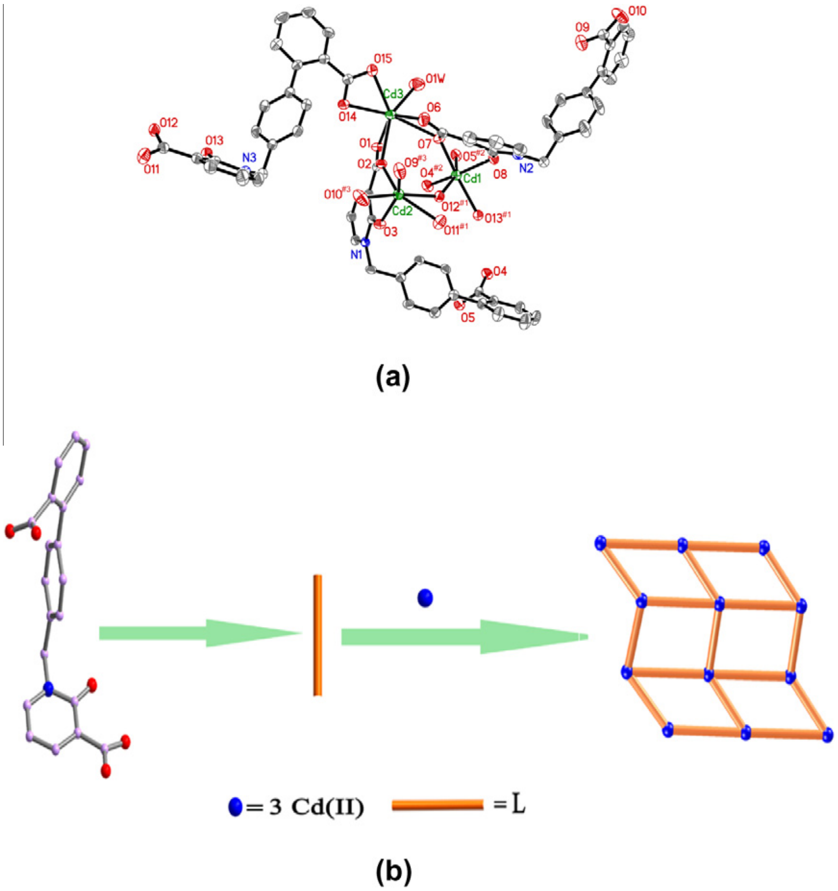

Fig. 9. (a) Coordination environments of the Cd(II) cations in **9** (30% probability displace ellipsoids). Symmetry codes: ${}^{\#1}x-1, y, z$; ${}^{\#2}-x+1, -y+1, -z+2$; ${}^{\#3}-x+1, -y, -z+1$; ${}^{\#4}x+1, y, z$. (b) Topological representation of the (4^4)-**sql** network.

3.1.8. Structure of [Cd(L)(phen)] (*8*)

As shown in Fig. 8a, the asymmetric unit **8** contains one Cd(II) cation, one phen ligand and one L anion. Each Cd(II) cation shows a distorted octahedral coordination geometry $\{CdN_2O_4\}$, surrounded by four oxygen atoms from three carboxylate and one phenolic hydroxyl of three L anions (Cd1–O1$^{\#2}$ = 2.325(3), Cd1–O2 = 2.257(3), Cd1–O3 = 2.405(2) and Cd1–O4$^{\#1}$ = 2.221(3) Å) and two nitrogen atoms from one phen ligand (Cd1–N2 = 2.325(3), Cd1–N3 = 2.342(3) Å). Each L anion in a μ_3-η^0:η^1:η^1:η^1:η^1 coordination mode (mode V, Scheme 2), links Cd(II) cations to generate a (4,4) sheet (Figs. 8b and S5). The phen ligands are decorated on two sides of the layer.

Furthermore, there exist intramolecular C31–H31···O1$^{\#5}$ and C3–H3···O5$^{\#4}$ hydrogen-bonding interactions between pyridine groups from phen ligands and carboxylate oxygen atoms from L anions. Besides, the methylene group of L anion donates H atom to O3 atom of phenolic hydroxyl group, generating intramolecular C7–H7B···O3 hydrogen-bonding interaction (Table S8b), which further stabilizes the 2D structure of **8** (Fig. 8c).

3.1.9. Structure of [Cd$_3$(L)$_3$(H$_2$O)]·2H$_2$O (*9*)

The asymmetric unit of **9** consists of three Cd(II) cations, three L anions, one coordinated water molecule and two lattice water molecules. As shown in Fig. 9a, Cd1 cation is six-coordinated by six oxygen atoms from three carboxylate and two phenolic hydroxyl of three L anions (Cd1–O = 2.251(3)–2.336(3) Å) in a trigonal prismatic [13] coordination environment. Cd2 cation is six-coordinated by six oxygen atoms from three L anions (Cd2–O = 2.214(3)–2.403(3) Å) in a distorted octahedral coordination geometry. Cd3 cation is seven-coordinated by six oxygen atoms from three L anions and one water molecule (Cd3–O 2.236(4)–2.640(3) Å) in slightly distorted pentagonal bipyramid coordination sphere. Each L anion in a μ_3-η^1:η^1:η^1:η^2:η^1 coordination mode (mode VI, Scheme 2) links three Cd(II) cations to form a wave-like layer (Fig. S6).

From a topological perspective, if three Cd(II) cations can be regarded as a 4-connected node, L anions can be considered as connectors, the layer can be described as a 4-connected (4,4) network (Fig. 9b).

3.1.10. Structure of [Cd$_3$(L)$_3$(biim-4)$_{0.5}$]·6H$_2$O (*10*)

As illustrated in Fig. 10a, the asymmetric unit of **10** contains three Cd(II) cations, half a biim-4 ligand, three L anions and six water molecules. Each Cd(II) cation is six-coordinated in a trigonal prismatic coordination environment. Cd1 is coordinated by six oxygen atoms from three carboxylates and two phenolic hydroxyl groups of three L anions. Cd1–O bond lengths vary from 2.245(4) to 2.313(5) Å. Cd2 is surrounded by five oxygen atoms from three carboxylate groups of three L anions (Cd2–O1 = 2.222(5), Cd2–O9$^{\#1}$ = 2.374(5), Cd2–O10$^{\#1}$ = 2.365(5), Cd2–O11$^{\#6}$ = 2.345(5), Cd2–O12$^{\#6}$ = 2.544(4) Å), and one nitrogen atom from one biim-4 ligand (Cd2–N4 = 2.253(6) Å). Cd3 is six-coordinated by six oxygen atoms from three carboxylates and one phenolic hydroxyl of three L anions. Cd3–O bond lengths are all within the normal range. As shown in Fig. 10b, three carboxylates link three Cd(II) cations to form a trinuclear unit. L anions bridge trinuclear units in μ_3-η^1:η^1:η^1:η^1:η^1 and μ_3-η^1:η^1:η^1:η^2:η^1 coordination modes (modes I and IV, Scheme 2) to generate a undulated layer. The layers are further linked by the biim-4 ligands to furnish a complicated 3D framework (Fig. 10c).

From a topological view, the trinuclear units can be considered as 5-connected nodes, and L anion and biim-4 ligand are regarded as linkers, respectively, the whole framework of **10** can be described as a 3D 5-connected net with the point symbol of $(4^6{\cdot}6^4)$.

3.2. Discussion

3.2.1. Effects of the N-donor ligands on the structures of the compounds

The N-donor ligands have a remarkable effect on the construction of the compounds. Compound $[Cd_3(L)_3(H_2O)]{\cdot}H_2O$ (**9**) shows a 2D network. However, when the N-donor ligands were introduced into the reaction system of **9**, structurally-different compounds **1**, **3**, **4**, **7**, **8** and **10** were obtained. For example, compounds $[Cd(L)(biim\text{-}6)_{0.5}]$ (**7**) and $[Cd_3(L)_3(biim\text{-}4)_{0.5}]{\cdot}6H_2O$ (**10**) display the effect of the lengths of the bis(imidazole) ligands on the structures. Compared with biim-4, biim-6 has a longer alkyl spacer. In **7**, the L anions bridge the Cd(II) cations to form an infinite double-chain. The chains are further linked by the biim-6 ligands to furnish a 2D 6^3-**hcb** network. Whereas, in **10**, the L anions link the Cd(II) cations to form layers, which are extended by the biim-4 ligands to generate a 3D framework with the $(4^6{\cdot}6^4)$ topology. Compounds **1** and **10** show the effects of the spacers on the structures. When two central carbon atoms of the biim-4 ligand are replaced by the phenyl group, a structurally different pbib ligand was obtained. In **1**, the L anions bridge the Cd(II) cations to yield an infinite double-chain. The chains are further linked by pbib ligands to furnish a layer. In **10**, the L anions bridge the Cd(II) cations to yield a undulated layer. The layers are further bridged by the biim-4 ligands to furnish a complicated 3D framework. Obviously, the phenyl group of the pbib ligand increases the steric hindrance when coordinated with the metal atoms.

When the rigid or chelating N-donor ligands were used, the compounds are inclined to form low dimensional structures [14]. Compounds **3**, **4** and **8** display the effects of chelating ligands on the structures. The introduction of pytp, tbpy and phen ligands hinders the propagation of metal–L linkages, and leads to 0D dimeric structure of compound **3**, an infinite chain structure of compound **4** and the (4,4) sheet of compound **8**. Compounds **2**, **5** and **6** also show the effect of the N-donor ligands on the structures of the complexes. Tack compounds $[Ni(L)(pbib)]{\cdot}2H_2O$ (**2**) and $[Ni(L)(tbpy)]{\cdot}0.25H_2O$ (**6**) for example. In **2**, the L anions bridge the Ni(II) cations to generate dimeric units, which are further linked by two kinds of pbib ligands to form a 2D network. While, in **6**, the L anions link the Ni(II) cations to generate an infinite helical chain. The tbpy ligands, as the dangling arms, are attached on both sides of the chain.

3.2.2. PXRD results and thermal analysis

To confirm whether the crystal structures are truly representative of the bulk materials, PXRD experiments were carried out for

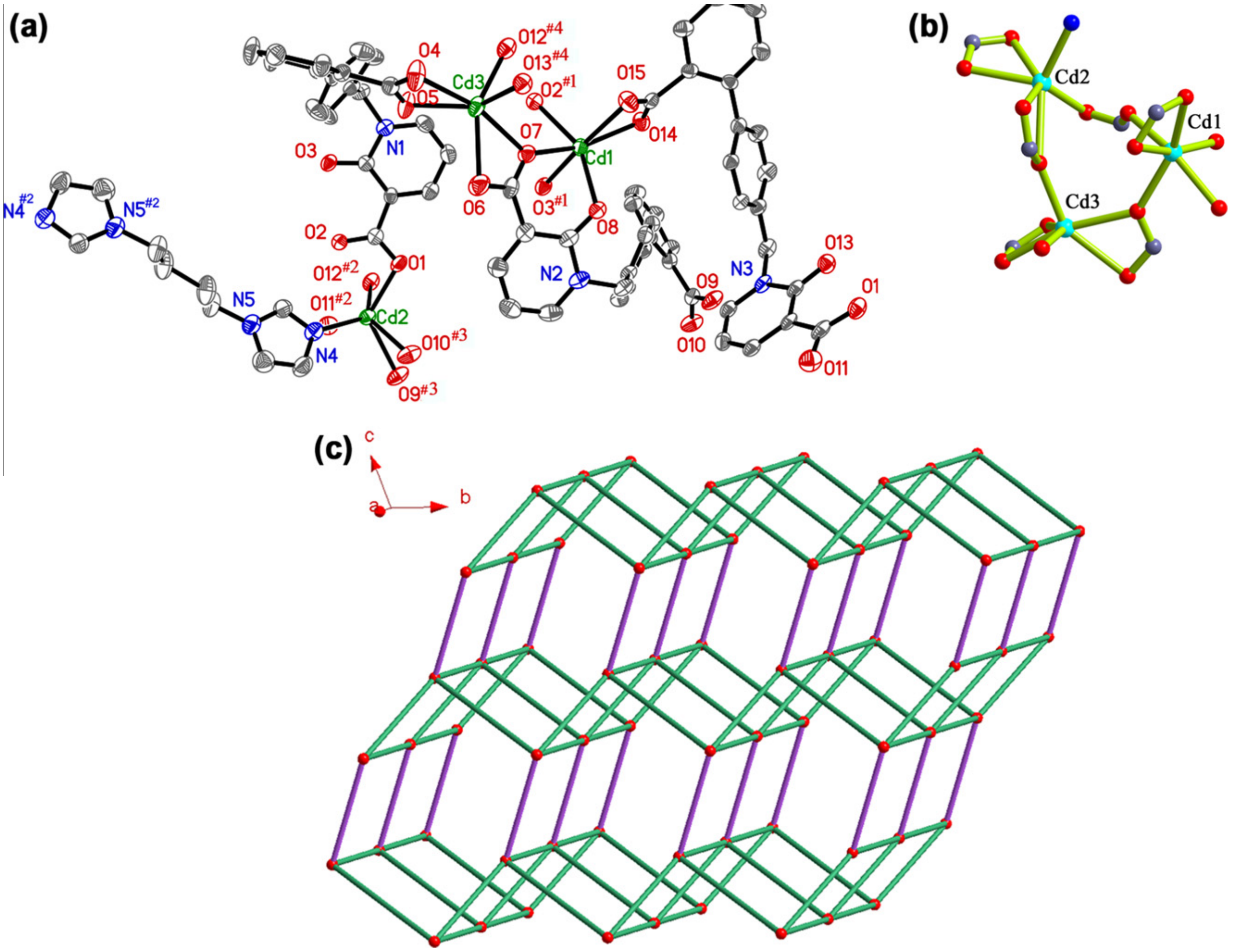

Fig. 10. (a) ORTEP view of **10** showing the local coordination environments of Cd(II) cations with hydrogen atoms omitted for clarity (30% probability displacement ellipsoids). Symmetry codes: #1 −x, −y − 1, −z; #2 x, y − 1, z − 1; #3 −x − 1, −y − 1, −z; #4 −x, −y, −z + 1; #5 −x, −y − 1, −z − 1; #6 x, y + 1, z + 1. (b) View of the trinuclear unit. (c) Topological representation of the 5-connected framework of **10**. In this network, red spheres represent trinuclear units, the purple and dark green lines represent the biim-4 ligands and L anions, respectively. (Color online.)

1–**10**. The PXRD experimental and computer-simulated patterns of the corresponding complexes are shown in the Supporting Information (Fig. S7). They show that the synthesized bulk materials and the measured single crystals are the same.

Thermogravimetric analyses were carried out for compounds **1**–**10** in order to characterize the compounds more fully in terms of thermal stability. The experiments were performed under N_2 atmosphere with a heating rate of 10 °C/min, as shown in Fig. S8 (see the Supporting Information). For compound **2**, the weight loss corresponding to the release of two lattice water molecules are observed from 33 to 127 °C (observed 6.2%, calculated 5.3%). The anhydrous compound begins to decompose at 351 °C. The remaining weight corresponds to the formation of NiO (observed 13.9%, calculated 11.0%). Compound **3** shows a 1.3% weight loss from 72 to 148 °C, corresponding to the loss of one free water molecule (calculated 1.2%). The second weight loss from 315 to 567 °C corresponds to the collapse of the framework. The remaining residue is 18.8%, which can be assigned to the formation of CdO (calculated 16.2%). Compound **6** loses its lattice water in the range of 53–93 °C (observed 0.7%, calculated 0.6%). After removal of the water molecules, the remaining solid is stable up to 394 °C. In the temperature range of 394–513 °C, the weight loss can be attributed to the decomposition of the organic ligand. The remaining weight corresponds to the formation of NiO (observed 10.4%, calculated 9.6%). For compound **9**, the weight loss corresponding to the release of the one lattice water molecule is observed from 50 to 76 °C (observed 1.4%, calculated 1.3%). The weight loss corresponding to the release of the one coordinated water molecule is observed from 161 to 175 °C (observed 1.5%, calculated 1.3%). Decomposition of the residual composition occurs from 348 to 536 °C, leading to the formation of CdO as the residue (observed 28.3%, calculated 27.2%). For **10**, the first weight loss corresponding to the release of water molecule is observed before 105 °C (observed 7.0%, calculated 6.8%). The departure of the organic components occurs from 311 °C (observed 27.13%, calculated 24.3%). For **1**, **4**, **5** and **8**, the decomposition of organic components occurs at 314–519, 315–534, 394–478 and 312–574 °C, respectively.

3.2.3. Luminescent properties

Luminescent properties of compounds with d^{10} metal centers have attracted much attention because of their potential applications in chemical sensors, photochemistry, and electroluminescent display [15]. Solid-state luminescent studies were carried out for ligands H_2L, phen, biim-4, biim-6, pbib, pytp and tbpy, as well as compounds **1**, **3**, **4** and **7**–**10** in the solid state at room temperature (Fig. S9 and Table 2). The emission bands for the free ligands are probably attributable to the $\pi^* \rightarrow n$ or $\pi^* \rightarrow \pi$ transitions [16].

The main emission peaks of biim-4, biim-6, phen and pbib [17] are at 438, 379, 380 and 423 nm, respectively. For pytp and tbpy, the emission peaks appear at 399 (λ_{ex} = 359 nm) and 401 nm (λ_{ex} = 308 nm). The H_2L shows an emission peak at 406 nm (λ_{ex} = 328 nm). The emission peaks of Cd(II)-containing compounds occur at 409 nm (λ_{ex} = 363 nm) for **1**, 414 nm (λ_{ex} = 286 nm) for **3**, 418 nm (λ_{ex} = 374 nm) for **4**, 403 nm (λ_{ex} = 309 nm) for **7**, 402 nm (λ_{ex} = 354 nm) for **8**, 403 nm (λ_{ex} = 324 nm) for **9** and 403 nm (λ_{ex} = 324 nm) for **10**. The emissions of compounds **1, 3, 4** and **7**–**10** are neither metal-to-ligand charge transfer (MLCT) nor ligand-to-metal charge transfer (LMCT) in nature since the Cd^{2+} cations are difficult to oxidize or to reduce because of their d^{10} configuration [18]. The emission peaks of compounds **1**, **3**, **4** and **7**–**10** should originate from the corresponding L anion, because similar emissions have been observed for the H_2L ligand [19,20].

Table 2
Photoluminescent data for **1**, **3**, **4**, **7–10** and organic ligands at room temperature.

Compounds	λ_{ex} (nm)	λ_{em} (nm)	Ligand	λ_{ex} (nm)	λ_{em} (nm)
1	366	409	biim-4	252	438
3	289	414	biim-6	343	379
4	400	418	phen	325	380
7	306	403	pbib	255	423
8	375	402	pytp	359	399
9	373	403	tbpy	308	401
10	371	403	H_2L	278	406

4. Conclusion

In summary, ten new coordination compounds were successfully synthesized under hydrothermal conditions by varying the N-donor ligands and central metals. These compounds display fascinating 0D, 1D, 2D and 3D structures. The structural differences of the compounds indicate that the organic ligands and the N-donor ligands have important effects on the resultant complex structures. The results also indicate that the H_2L ligand is a good candidate for the construction of coordination compounds with aesthetic structures. The photoluminescent emissions indicate that compounds **1**, **3**, **4** and **7**–**10** may be good candidates for optical materials.

Acknowledgments

We thank the National Natural Science Foundation of China (Grant Nos. 21071028, 21001023, 21277022), the Science Foundation of Jilin Province (201215005, 20100109) and the Fundamental Research Funds for the Central Universities for support.

Appendix A. Supplementary material

Selected bond lengths and angles, PXRD patterns, thermogravimetric (TG) of the compounds **1**–**6** and **8**–**10**, emission spectra of the H_2L and the N-donor ligands are given in Supplementary Information. CCDC 884320–884329 contain the supplementary crystallographic data for compounds **1**–**10**. These data can be obtained free of charge via http://www.ccdc.cam.ac.uk/conts/retrieving.html, or from the Cambridge Crystallographic Data Centre, 12 Union Road, Cambridge CB2 1EZ, UK; fax: +44 1223-336-033; or e-mail: deposit@ccdc.cam.ac.uk. Supplementary data associated with this article can be found, in the online version, at http://dx.doi.org/10.1016/j.poly.2012.11.045.

References

[1] (a) A. Erxleben, Coord. Chem. Rev. 246 (2003) 203;
(b) G. Ferey, C.Mellot. Draznieks, C. Serre, F. Millange, Acc. Chem. Res. 38 (2005) 217;
(c) L. Pan, D.H. Olson, L.R. Ciemnolonski, R. Heddy, J. Li, Angew. Chem., Int. Ed. 45 (2006) 616;
(d) S.L. James, Chem. Soc. Rev. 32 (2003) 276;
(e) Q. Wang, R. Yang, C.F. Zhuang, J.Y. Zhang, B.S. Kang, C.Y. Su, Eur. J. Inorg. Chem. (2008) 1702;
(f) H.L. Jiang, Y. Tatsu, Z.H. Lu, Q. Xu, J. Am. Chem. Soc. 132 (2010) 5586;
(g) H.L. Jiang, Q. Xu, Chem. Commun. 47 (2011) 3351;
(h) H.L. Jiang, T. Akita, T. Ishida, M. Haruta, Q. Xu, J. Am. Chem. Soc. 133 (2011) 1304;
(i) H. Wu, H.Y. Liu, J. Yang, B. Liu, J.F. Ma, Y.Y. Liu, Y.Y. Liu, Cryst. Growth Des. 11 (2011) 2317;
(i) W.Q. Kan, J.F. Ma, Y.Y. Liu, J. Yang, CrystEngComm 14 (2012) 2316;
(j) C. Janiak, J.K. Vieth, New J. Chem. 34 (2010) 2366;
(k) C.B. Aakeröy, N.R. Champness, C. Janiak, CrystEngComm 12 (2010) 22.
[2] (a) K. Adachi, Y. Sugiyama, K. Yoneda, K. Yamada, K. Nozaki, A. Fuyuhiro, S. Kawata, Chem. Eur. J. 11 (2005) 6616;
(b) T. Lee, M.S. Lin, Cryst. Growth Des. 7 (2007) 1803;
(c) J. Pasan, J. Sanchiz, F. Lloret, M. Julve, C. Ruiz-Perez, CrystEngComm 9 (2007) 478;
(d) L.F. Ma, Y.Y. Wang, L.Y. Wang, J.Q. Liu, Y.P. Wu, J.G. Wang, Q.Z. Shi, S.M. Peng, Eur. J. Inorg. Chem. (2008) 693;
(e) W.Q. Kan, J.F. Ma, B. Liu, J. Yang, CrystEngComm 14 (2012) 286.
[3] M. Munakata, L.P. Wu, T. Kuroda, Inorg. Chem. 36 (1997) 5416;
(a) X.H. Bu, W. Chen, W.F. Hou, M. Du, R.H. Zhang, F. Brisse, Inorg. Chem. 41

(2002) 3477;
(b) Y.Y. Liu, J.F. Ma, J. Yang, Z.M. Su, Inorg. Chem. 46 (2007) 3027;
(c) J. Yang, J.F. Ma, Y.Y. Liu, J.C. Ma, S.R. Batten, Cryst. Growth Des. 8 (2008) 4383;
(d) L.P. Zhang, J.F. Ma, J. Yang, Y.Y. Liu, G.H. Wei, Cryst. Growth Des. 9 (2009) 4660;
(e) K.A. Hirsch, S.R. Wilson, J.S. Moore, Inorg. Chem. 36 (1997) 2960;
(f) W.H. Zhang, Y.Y. Wang, E.K. Lermontova, G.P. Yang, B. Liu, J.C. Jin, Z. Dong, Q.Z. Shi, Cryst. Growth Des. 10 (2010) 76;
(g) L.F. Ma, L.Y. Wang, J.L. Hu, Y.Y. Wang, G.P. Yang, Cryst. Growth Des. 9 (2009) 5334;
(h) Y.Y. Liu, Z.H. Wang, J. Yang, B. Liu, Y.Y. Liu, J.F. Ma, CrystEngComm 13 (2011) 3811;
(i) W.Q. Kan, Y.Y. Liu, J. Yang, Y.Y. Liu, J.F. Ma, CrystEngComm 13 (2011) 4256.

[4] (a) C. Janiak, Dalton Trans. (2003) 2781;
(b) O.R. Evans, W. Lin, Acc. Chem. Res. 35 (2002) 511;
(c) N.W. Ockwig, O. Delgado-Friedrichs, M. O'Keeffe, O.M. Yaghi, Acc. Chem. Res. 38 (2005) 176;
(d) S.R. Batten, R. Robson, Angew. Chem., Int. Ed. 37 (1998) 1460;
(e) C.N.R. Rao, S. Natarajan, R. Vaidhy-anathan, Angew. Chem., Int. Ed. 43 (2004) 1466;
(f) S. Kitagawa, R. Kitaura, S.I. Noro, Angew. Chem., Int. Ed. 43 (2004) 2334;
(g) V.A. Blatov, L. Carlucci, G. Ciani, D.M. Proserpio, CrystEngComm 6 (2004) 378;
(h) M.H. Hu, G.L. Shen, J.X. Zhang, Y.G. Yin, D. Li, Cryst. Growth Des. 9 (2009) 4533;
(i) L.L. Wen, F. Wang, J. Feng, K.L. Lv, C.G. Wang, D.F. Li, Cryst. Growth Des. 9 (2009) 3581;
(j) H.Y. Bai, J.F. Ma, J. Yang, L.P. Zhang, J.C. Ma, Y.Y. Liu, Cryst. Growth Des. 10 (2010) 1946;
(k) W.Q. Kan, J. Yang, Y.Y. Liu, J.F. Ma, Polyhedron 30 (2011) 2113.

[5] (a) T.M. Reineke, M. Eddaoudi, D. Moler, M. O'Keeffe, O.M. Yaghi, J. Am. Chem. Soc. 122 (2000) 4843;
(b) X. Guo, G. Zhu, Z. Li, F. Sun, Z. Yang, S. Qiu, Chem. Commun. (2006) 3172;
(c) S.N. Wang, J.F. Bai, H. Xing, Y.Z. Li, Y. Song, Y. Pan, M. Scheer, X.Z. You, Cryst. Growth Des. 7 (2007) 747;
(d) Q.R. Fang, G.S. Zhu, M. Xue, Q.L. Zhang, J.Y. Sun, X.D. Guo, S.L. Qiu, S.T. Xu, P. Wang, D.J. Wang, Y. Wei, Chem. Eur. J. 12 (2006) 3754;
(e) Z.R. Pan, H.G. Zheng, T.W. Wang, Y. Song, Y.Z. Li, Z.J. Guo, S.R. Batten, Inorg. Chem. 47 (2008) 9528;
(f) J. Yang, J.F. Ma, Y.Y. Liu, J.C. Ma, S.R. Batten, Inorg. Chem. 46 (2007) 6542;
(g) L.P. Zhang, J. Yang, J.F. Ma, Z.F. Jia, Y.P. Xie, G.H. Wei, CrystEngComm 10 (2008) 1410.

[6] (a) S.O.H. Gutschke, D.J. Price, A.K. Powell, P.T. Wood, Angew. Chem., Int. Ed. 40 (2001) 1920;
(b) S.K. Ghosh, P.K. Bharadwaj, Inorg. Chem. 43 (2004) 5180;
(c) J. Zhang, Y.B. Chen, S.M. Chen, Z.J. Li, J.K. Cheng, Y.G. Yao, Inorg. Chem. 45 (2006) 3161.

[7] (a) X.J. Wang, M.X. Jiang, C.H. Zhang, Y.L. Feng, Y.H. He, J. Struct. Chem. 30 (2011) 36;
(b) C.H. Zhang, M.X. Jiang, Y.L. Feng, Y.H. He, Polyhedron 29 (2010) 2250;
(c) H.A. Habib, Inorg. Chim. Acta 362 (2009) 2452;
(d) H.A. Habib, H. Anke, H.A. Höppe, C. Janiak, Dalton Trans. (2009) 1742;
(e) H.A. Habib, J. Sanchizb, C. Janiak, Dalton Trans. (2008) 1734;
(f) B. Wisser, Y. Lu, C. Janiak, Z. Anorg. Allg. Chem. 633 (2007) 1189.

[8] (a) H.A. Habib, H. Anke, H.A. Höppe, G. Steinfeld, C. Janiak, Inorg. Chem. 48 (2009) 2166;
(b) K.S. Henninger, H.A. Habib, C. Janiak, J. Am. Chem. Soc. 131 (2009) 2776;
(c) P.P. Yang, B. Li, Y.H. Wang, W. Gu, X. Liu, Z. Anorg. Allg. Chem. 634 (2008) 1210;
(d) J. Yang, J.F. Ma, Y.Y. Liu, S.R. Batten, CrystEngComm 11 (2009) 151;
(e) M. Du, Z.H. Zhang, X.G. Wang, L.F. Tang, X.J. Zhao, CrystEngComm 10 (2008) 1855.

[9] Y.H. He, Y.L. Feng, Y.Z. Lan, Y.H. Wen, Cryst. Growth Des. 8 (2008) 3586.

[10] (a) S.L. Li, Y.Q. Lan, J.F. Ma, J. Yang, J. Wei, L.P. Zhang, Z.M. Su, Cryst. Growth Des. 8 (2008) 675;
(b) J. Yang, J.F. Ma, Y.Y. Liu, S.L. Li, G.L. Zheng, Eur. J. Inorg. Chem. (2005) 2174;
(c) Y.Y. Liu, J.F. Ma, J. Yang, J.C. Ma, Z.M. Su, CrystEngComm 10 (2008) 894;
(d) J. Yang, J.F. Ma, Y.Y. Liu, J.C. Ma, H.Q. Jia, N.H. Hu, Eur. J. Inorg. Chem. 6 (2006) 1208;
(e) F.F. Li, J.F. Ma, S.Y. Song, J. Yang, Y.Y. Liu, Z.M. Su, Inorg. Chem. 44 (2005) 9374;
(f) A.M.W. Cargill Thompson, Coord. Chem. Rev. 160 (1997) 1;
(g) G.W.V. Cave, C.L. Raston, Chem. Commun. (2000) 2199.

[11] (a) G.M. Sheldrick, SHELXS-97, Programs for X-ray Crystal Structure Solution, University of Göttingen, Göttingen, Germany, 1997;
(b) G.M. Sheldrick, SHELXL-97, Programs for X-ray Crystal Structure Refinement, University of Göttingen, Göttingen, Germany, 1997;
(c) L.J. Farrugia, WINGX, A Windows Program for Crystal Structure Analysis, University of Glasgow, Glasgow, UK, 1988.

[12] J. Christoph, J. Chem. Soc., Dalton Trans. (2000) 3885.

[13] (a) S. Banerjee, A. Ghosh, B. Wu, P.G. Lassahn, C. Janiak, Polyhedron 24 (2005) 593;
(b) S. Banerjee, P.G. Lassahn, C. Janiak, A. Ghosh, Polyhedron 24 (2005) 2963.

[14] (a) M. Khanpour, A. Morsali, P. Retailleau, Polyhedron 29 (2010) 1520;
(b) Y.G. Li, Q. Wu, L. Lecren, R. Clérac, J. Mol. Struct. 890 (2008) 339;
(c) J. Astner, M. Weitzer, S.P. Foxon, S. Schindler, F.W. Heinemann, J. Mukherjee, R. Gupta, V. Mahadevan, R. Mukherjee, Inorg. Chim. Acta 361 (2008) 279;
(d) L. Hashemi, A. Morsali, P. Retailleau, Inorg. Chim. Acta 367 (2011) 207.

[15] (a) J.E. McGarrah, Y.J. Kim, M. Hissler, R. Eisenberg, Inorg. Chem. 40 (2001) 4510;
(b) Q. Wu, M. Esteghamatian, N.X. Hu, Z. Popovic, G. Enright, Y. Tao, M. D'Iorio, S. Wang, Chem. Mater. 12 (2000) 79;
(c) G.D. Santis, L. Fabbrizzi, M. Licchelli, A. Poggi, A. Taglietti, Angew. Chem., Int. Ed. Engl. 35 (1996) 202.

[16] (a) X. Shi, G. Zhu, Q. Fang, G. Wu, G. Tian, R. Wang, D. Zhang, M. Xue, S. Qiu, Eur. J. Inorg. Chem. (2004) 185;
(b) G. Tian, G.S. Zhu, Q.R. Fang, X.D. Guo, M. Xue, J.Y. Sun, S.L. Qiu, J. Mol. Struct. 787 (2006) 45.

[17] (a) L.P. Zhang, J.F. Ma, J. Yang, Y.Y. Pang, J.C. Ma, Inorg. Chem. 49 (2009) 1535;
(b) X.M. Zhang, M.L. Tong, M.L. Gong, X.M. Chen, Eur. J. Inorg. Chem. (2003) 138.

[18] (a) L. Wen, Y. Li, Z. Lu, J. Lin, C. Duan, Q. Meng, Cryst. Growth Des. 6 (2006) 530;
(b) L. Wen, Z. Lu, J. Lin, Z. Tian, H. Zhu, Q. Meng, Cryst. Growth Des. 7 (2007) 93;
(c) J.G. Lin, S.Q. Zang, Z.F. Tian, Y.Z. Li, Y.Y. Xu, H.Z. Zhu, Q.J. Meng, CrystEngComm 9 (2007) 915;
(d) S.L. Zheng, X.M. Chen, Aust. J. Chem. 57 (2004) 703.

[19] (a) Z.F. Chen, R.G. Xiong, J. Zhang, X.T. Chen, Z.L. Xue, X.Z. You, Inorg. Chem. 40 (2001) 4075;
(b) J.C. Dai, X.T. Wu, Z.Y. Fu, C.P. Cui, S.M. Hu, W.X. Du, L.M. Wu, H.H. Zhang, R.O. Sun, Inorg. Chem. 41 (2002) 1391;
(c) (c) A. Thirumurugan, S. Natarajan, J. Chem. Soc., Dalton Trans. (2004) 2923.

[20] J.F. Ma, J. Yang, S.L. Li, S.Y. Song, Cryst. Growth Des. 5 (2005) 807.